# Time-Resolved Resonance Raman Study of HbA with 220 nm Excitation: Probing Phenylalanine

**Janina Kneipp, Gurusamy Balakrishnan, and Thomas G. Spiro***

*Department of Chemistry, Princeton University, Princeton, New Jersey 08544*

*Received: May 18, 2004; In Final Form: July 30, 2004*

This study explores different UV wavelengths for the resonant Raman excitation of hemoglobin in its two affinity states (T and R). Changes in the T − R difference spectra as a function of excitation wavelength are reported and discussed in context with the excitation profiles of UV resonance Raman bands in the T and the R states. Excitation with 220 nm results in difference signals of the phenylalanine modes F8a and F8b and changes in tryptophan modes associated with the tryptophan residues $\alpha 14/\beta 15$ in the difference spectra. To explore the time-dependent behavior of these changes, we conducted pump−probe experiments and used 220 nm excitation to monitor differences between the photocycle intermediates and HbCO. We found differences in the F8a and F8b modes as early as 40 ns after deligation. These results suggest that phenylalanine residues in close proximity of the heme are probed. In addition, a negative band for the W3 component associated with the $\alpha 14/\beta 15$ tryptophan residues between UVRR spectra of the T and the R states suggests differences in hydrogen bonding of the internal tryptophan residues.

## 1. Introduction

Hemoglobin (Hb) is a well-studied molecule that plays an important role in the effort to understand allosteric mechanisms in proteins. Upon ligand binding, Hb undergoes a change in tertiary and quaternary structure, thereby controlling cooperativity of the binding process. To understand the dynamics of this process, Hb molecules have been monitored by transient absorption, fluorescence, and vibrational spectroscopic methods while they undergo deligation and subsequent rebinding of a ligand. Resonance Raman (RR) spectroscopy is a powerful method to study structural changes in Hb. It enables probing of selectively enhanced parts of the molecule by varying excitation wavelength and thus provides different perspectives on the deligation/religation process. Extensive UVRR studies on HbA as well as mutant rHbs[1−8] have shed new light on the mechanics of the molecule and its motion through breaking and reforming of H bonds and salt bridges after photodeligation of CO. Time-resolved UVRR photodeligation experiments are usually done in a "classical" pump−probe setting, where one laser pulse at the wavelength of the Soret absorption maximum (419 nm) is used to remove the ligand from the heme and a second laser excites Raman scattering after a defined time interval (delay). Recently, a new intermediate in the Hb photocycle was identified by time-resolved UVRR spectroscopy with 229 nm excitation.[9]

In the study presented here, we explore excitation wavelengths below 229 nm to probe different side chains in the Hb molecule and to look for additional differences between the two Hb affinity states T (unligated) and R (CO-bound form). We found strong enhancement of phenylalanine bands together with interesting signals from the internal tryptophan residues for excitation at 220 nm and conducted time-resolved pump−probe experiments at this wavelength. Time-resolved experiments at a similar excitation wavelength (218 nm) were reported by Kaminaka et al.[10] Their study focused on the microsecond time scale (delay times 10−500 $\mu$s), and reported no change in the UVRR bands before 10−20 $\mu$s with differences for some tryptophan modes at the long delay times (10−100 $\mu$s).[10] Having expanded our understanding of the Hb photocycle to the nanosecond time scale, we now know that by 10 $\mu$s after photodeligation, the Hb molecules have undergone three intermediate states with characteristic UVRR spectral signatures as characterized by pump−probe experiments with 229 nm excitation.[9] Our UVRR experiment allowed the collection of good signal-to-noise spectra, permitting the utilization of difference spectra even for the relatively small spectral differences found with 220 nm excitation. In this paper, we discuss and interpret 220 nm time-resolved UVRR data in the context of our current picture of the HbCO photocycle.

## 2. Experimental Section

HbA was prepared from fresh human blood by standard procedures[11] and the CO adduct was stored frozen in CO-saturated buffer. Before the experiments, HbA was thawed and exchanged into 50 mM sodium phosphate buffer saturated in CO (pH 7.4) using Centricon concentrators by three 40 min centrifuge cycles. The concentration of the final HbCO samples was 0.3−0.4 mM in heme as determined by absorption spectroscopy. The CO-saturated phosphate buffer contained 0.2 M sodium perchlorate as the internal intensity standard. Acetone or cyclohexane was used for frequency calibration.

The Hb(deoxy) sample was prepared by purging sealed vials containing HbCO with $N_2$ for 1 h and subsequent irradiation with visible light under constant $N_2$ flow for 2 h.

Raman measurements were carried out in quartz NMR tubes spinning around a stirring wire made of stainless steel to mix the sample. The outside of the spinning NMR tube was cooled by dry air that had been directed through copper tubing embedded in dry ice. CO was directed onto the surface of the HbCO solution during the whole time of the measurements.

* Address for correspondence: Prof. Thomas G. Spiro, Department of Chemistry, Princeton University, Princeton, NJ 08544. Phone: (609) 258 3907. Fax: (609) 258 0348, E-mail: spiro@princeton.edu.

10.1021/jp047848k CCC: $27.50 
Published on Web 09/14/2004

During acquisition of spectra from Hb(deoxy), the CO flow was replaced by $N_2$. The spinning speed was adjusted to 400−600 rpm and monitored using a tachometer. Measurements at low excitation wavelengths were carried out in an airtight, wire-guided flow cell with a quartz front window. The cell was purged by $N_2$ and CO for measurements on Hb(deoxy) and Hb(CO), respectively, and the sample solution was kept in a cooled, $N_2$/CO-purged reservoir and moved through the cell with a peristaltic pump.

For the resonance Raman experiments we used a system of two tunable Ti:Sapphire lasers, both pumped by intracavity frequency-doubled (527 nm) Nd:YLF lasers (GM30/Photonics International Inc.), described before.[12] To generate a 419 nm pump pulse (∼25 ns at 1 kHz, ∼65 $\mu$J/pulse), light from one of the Ti:Sapphire lasers (838 nm) was frequency doubled. The 220 nm probe pulse (∼25 ns at 1 kHz, 0.5−0.6 $\mu$J/pulse) was generated by quadrupling the 880 nm output of the second Ti:Sapphire laser. Pump and probe laser beams were focused onto the sample by two cylindrical quartz lenses and the spots were spatially overlapping on the surface of the sample tube. The scattered light was collected with a pair of quartz lenses in 135° backscatter geometry and imaged onto a Spex 1269 spectrograph (1.26 m, grating 3600 grooves/mm) equipped with a liquid nitrogen-cooled CCD camera (Roper Scientific).

Static Hb(deoxy) and HbCO were measured in the absence of the pump laser beam by tuning the probe laser to different wavelengths between 206 and 229 nm. Laser light at 195 nm was generated by frequency mixing of the first and third harmonic of the Ti: Sapphire output.

For the time-resolved experiments carried out at 220 nm excitation, the pump beam was adjusted to yield maximum photolysis in the sample, which was verified by examining the $\nu_4$ CO-heme Raman band intensity at 1372 cm$^{-1}$ with the 419 nm pump light exciting into the Soret region. We observed that the intensity of the $\nu_4$ band associated with the CO-bound heme (at 1372 cm$^{-1}$) was minimized and at the same time the $\nu_4$ signal of deoxy heme (1354 cm$^{-1}$) increased to a maximum. This indicates that the protein is fully deligated by the pump pulse. Both lasers were controlled with a delay generator (DG535, Stanford Research Systems) via a GPIB interface, so that the delay between pump and probe pulse could be set in the data acquisition software. Raman spectra were collected for 14 different delay times of the probe beam (probe after pump: 40 ns, 60 ns, 100 ns, 250 ns, 400 ns, 600 ns, 1 $\mu$s, 2.5 $\mu$s, 6 $\mu$s, 20 $\mu$s, 50 $\mu$s, 100 $\mu$s, and 200 $\mu$s). In each experiment a probe-only spectrum (without pump pulse) was acquired 600 ns before the pump pulse. Acquisition of each signal (probe only and pump−probe) was switched every 30 s (paired readout) for a duration of 20 min per sample, yielding average signals of 10 min for the probe-before-pump and probe-after-pump sequences, respectively. The sample was then exchanged. The final spectra of each delay time were results of averages of 14 to 16 10 min measurements. For analysis, spectra acquired at the different time delays were scaled by assuming identical probe-only (HbCO) spectra for all experiments. The differences between pump−probe and probe only spectra were calculated for each delay time based on the band of sodium perchlorate (934 cm$^{-1}$) as the internal standard. The perchlorate intensity standard was also used to calculate all static difference spectra.

## 3. Results and Discussion

**3.1. T − R Difference Variation with Excitation Wavelength.** RR spectra with 229 nm excitation have proven to be very useful for studies of Hb dynamics, since they provide information on aromatic residues involved in the formation of tertiary and quaternary contacts that differ in the ligand-bound and unliganded state of the Hb molecule.[1,2,4,9] These contacts cause differences in scattering intensity as well as frequency shifts, producing a difference spectrum between unbound and CO-bound hemoglobin.

To probe different parts of the Hb molecule, we explored a number of different excitation wavelengths below 229 nm and compared T and R state spectra. To interpret the T − R differences, we will discuss the change of cross-section with excitation wavelength for selected bands in the T state and compare them to those of the R state. Such excitation profiles are known for the aromatic amino acids in solution from a number of studies.[13−15] Recently, they also have been established for hemoglobin in the R state.[12]

As expected for the altered resonance conditions for different residues, the overall pattern of the hemoglobin spectra changes drastically as excitation wavelength is changed, and cross-sections of CO-bound and unbound hemoglobin are altered. As a result, the T − R differences change, as will be discussed in the following sections.

*195 nm.* Phenylalanine modes at 1003 cm$^{-1}$ (F12), 1030 cm$^{-1}$ (F18a), and 1207 cm$^{-1}$ ($C_6H_5$–C stretching)[16] are strongly enhanced in the 195 nm spectrum, which otherwise mainly contains broad amide bands and F8a/F8b modes of similar intensity (Figure 1). As reported by Fodor et al.[14] the 1003 cm$^{-1}$ and 1207 cm$^{-1}$ phenylalanine bands are more than an order of magnitude stronger than when excited around 200 nm. The F8a/F8b modes overlap with Y8a/Y8b, producing broad features at 1615 cm$^{-1}$/1590 cm$^{-1}$. Despite the strong resonance enhancement of many bands, the difference spectrum is weak, indicating little effect of the altered Hb structure.

Interestingly, we find a T − R difference in the tyrosine Fermi doublet at 848/823 cm$^{-1}$. The doublet is due to resonance between the symmetric ring-breathing $\nu_1$ and the overtone $2\nu_{16a}$ of the nonplanar ring vibration at 413 cm$^{-1}$.[17] Strong UV resonance enhancement of these bands in aqueous solution of neutral pH was reported for 200 and 240 nm excitation, but not for 218 nm.[16] The fact that the hemoglobin T state spectra of Figure 1 do not display the band pair with excitation at 206 nm and above is consistent with this earlier observation. The intensity ratio of 848/823 cm$^{-1}$ is 10:9 in the Hb(deoxy) spectrum and 7:10 in the HbCO spectrum, resulting in a negative T − R difference at 823 cm$^{-1}$. Effects such as this have previously been discussed in terms of changes in hydrogen bonds and ionization of the hydroxyl group.[17] Interpretation of the 848/823 cm$^{-1}$ ratio was attempted for some proteins[18,19] based on systematic studies of tyrosine and similar model compounds in different solvents and varying pH with Raman excitation in the visible [17] and UV.[16] The ratio of 0.7 in the HbCO (R state) spectrum can be interpreted as resulting from an increase in negative charge at the hydroxyl oxygen. It, thus, indicates that the phenolic hydroxyl group is solvent exposed, ionized, or strongly hydrogen bonded.[17] The band ratio of 1.1 as seen in the Hb(deoxy) state suggests that tyrosine is moderately H bonded. We know that the tyrosine residues at the $\alpha_1\beta_2$ subunit interfaces ($\alpha$42) form a stronger bond in the T state than in the R state, where they interact with water molecules. The lower $I_{(848)}/I_{(823)}$ ratio in the R state could be explained by the altered solvent exposure of tyrosine $\alpha$42 or other, solvent-exposed tyrosine residues. Work by Hildebrandt et al.[18] also showed that not only H bonds, but other environmental effects such as hydrophobic residues surrounding the tyrosine, affect the intensity ratio of the Fermi doublet.

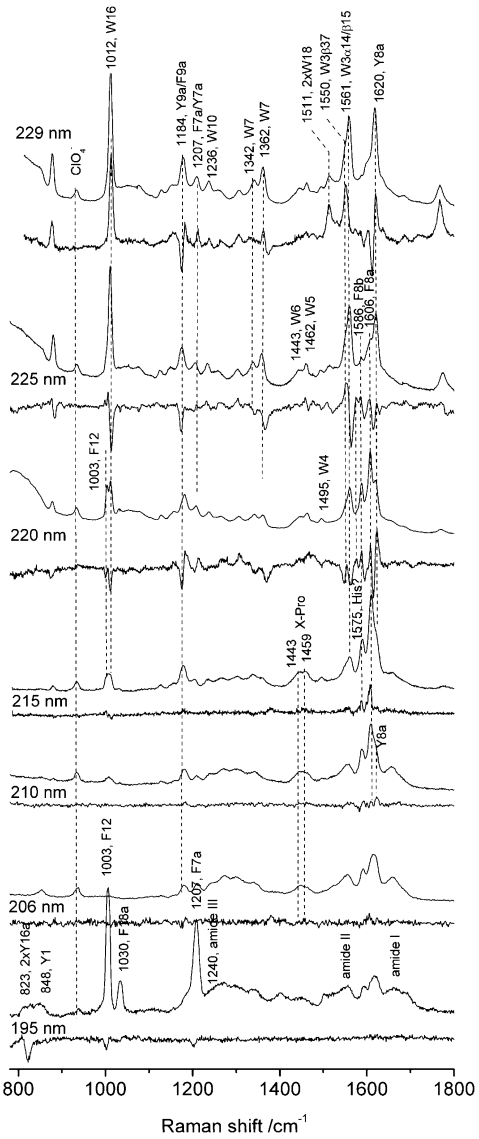


**Figure 1.** Resonance Raman spectra of Hb(deoxy) (T state), acquired with different excitation wavelengths, and the corresponding difference spectra of Hb(deoxy) and HbCO (T state spectrum minus R state spectrum) for the indicated seven excitation wavelengths between 195 and 229 nm.

The amide signals, which are strongly enhanced with 195 nm excitation in the parent spectra, are the same for the T and the R states. This is consistent with the fact that, while the molecule undergoes tertiary and quaternary changes during the transition from T to R, its mainly α-helical secondary structure remains unchanged. Time-resolved studies with FTIR spectroscopy were able to monitor changes in single amide bonds. They also produced evidence for the breaking and reforming of the interhelical H bonds between Valα93/$\beta$95 and Tyrα140/$\beta$145 during the R−T transition from shifts of the amide I frequency.[20] However, the accuracy of the UVRR measurements is insufficient to observe changes at the single residue level in the amide region; large improvement in the signal-to-noise ratio of the parent UVRR spectra would be required. As will be discussed later, UVRR can, however, also monitor the breaking and reforming of individual tyrosine H bonds.[9]

*206−215 nm.* With longer wavelength excitation, the strong phenylalanine contributions from F12 and F18a diminish and the W3 tryptophan mode begins to replace the amide II mode. Also, the amide I and III modes become weaker as the excitation wavelength moves further from resonance. At 206 to 215 nm excitation, the X-Proline amide II band (1450 $cm^{-1}$) is visible very clearly in the parent spectra. Both tyrosine and phenylalanine contribute to the band at 1184 $cm^{-1}$ (Y9a and F9a). Although a slight change of the Y9a/F9a band is found in almost all low-wavelength spectra (from 206 nm up), it only starts to become pronounced with 220 nm excitation. Similarly, the band at 1207 $cm^{-1}$ results from contributions of phenylalanine (F7a) and tyrosine (Y7a). The T − R differences remain very weak until 210 nm, where features due to a Y8a tyrosine upshift in the T state and positive phenylalanine bands become visible (F8a and F8b). The excitation profiles of these bands (Figure 2) also reflect these differences.

The fact that the X-proline bonds can be detected due to their shifted amide II frequency without much interference from other bands, along with the good resonance enhancement, enables monitoring of changes in H bond strength of the X-proline carbonyl.[21] We see a slightly positive difference feature at 1459 $cm^{-1}$ for X-proline with 206 and 210 nm excitation, although it appears weaker than the one reported in earlier studies with 212 nm.[22] Since the frequency of the X-proline band increases with H bond strength,[21] the positive difference at the high-frequency position (1459 $cm^{-1}$) of the broad X-proline band indicates stronger H bonding of proline in the T state. Zhao et al.[22] provided a detailed comparison of their UVRR results obtained with 212 nm excitation and the crystal structure data, which show that in the T state more X-proline carbonyls form H bonds. Furthermore, a positive difference band is seen around 1575 $cm^{-1}$ that is difficult to assign but has been suggested to originate from a histidine mode that becomes more enhanced in the T state.[22]

The phenylalanine bands become very pronounced with 215 nm excitation (Figure 1), and the excitation profile of the F8a mode shows a maximum for this wavelength (Figure 2). Compared to the cross-sections reported for phenylalanine in aqueous solution,[14] the excitation profile of F8a in hemoglobin is slightly red shifted. The total cross-section per molecule is in good agreement with that observed for aqueous phenylalanine[14] and for phenylalanine in HbCO.[12] It should be noted here that overlap of the F8a mode with the tyrosine Y8a mode in the hemoglobin spectra may introduce some uncertainty in the determination of the F8a cross-sections. The excitation profile illustrates the positive difference between the T state and the R state for the F8a mode, which dominates the T − R spectra together with F8b (1607 and 1587 $cm^{-1}$, respectively, see Figure 1). Amide contributions except those from amide II of X-proline have almost disappeared in the Hb spectrum at 215 nm excitation. The tryptophan W5 (1462 $cm^{-1}$) and W6 (1443 $cm^{-1}$) modes overlap with the X-proline band, and the W7 Fermi doublet (1360/1342 $cm^{-1}$) becomes visible.

*220−229 nm.* In this wavelength region, we observe strong enhancement of the tryptophan and tyrosine modes in Hb. In addition, the increasing cross-section of the phenylalanine bands with decreased excitation wavelength (Figure 2) results in significant contributions of this amino acid to the Hb spectra.

The RR spectrum with 229 nm excitation, as well as the corresponding difference spectrum (Figure 1) between the T and R states, are well known and have been discussed and interpreted in many previous studies.[1,23,24]

Excitation at 220 nm reveals clear phenylalanine features in the region between 1580 and 1620 $cm^{-1}$, with tyrosine Y8a and tryptophan W1 producing a 1619 $cm^{-1}$ shoulder. In addition, the phenylalanine F12 signal (1003 $cm^{-1}$) reaches the same intensity as that of W16 (1012 $cm^{-1}$) in the parent spectra (Figure 1). Deconvolution of the bands clarifies the contribution

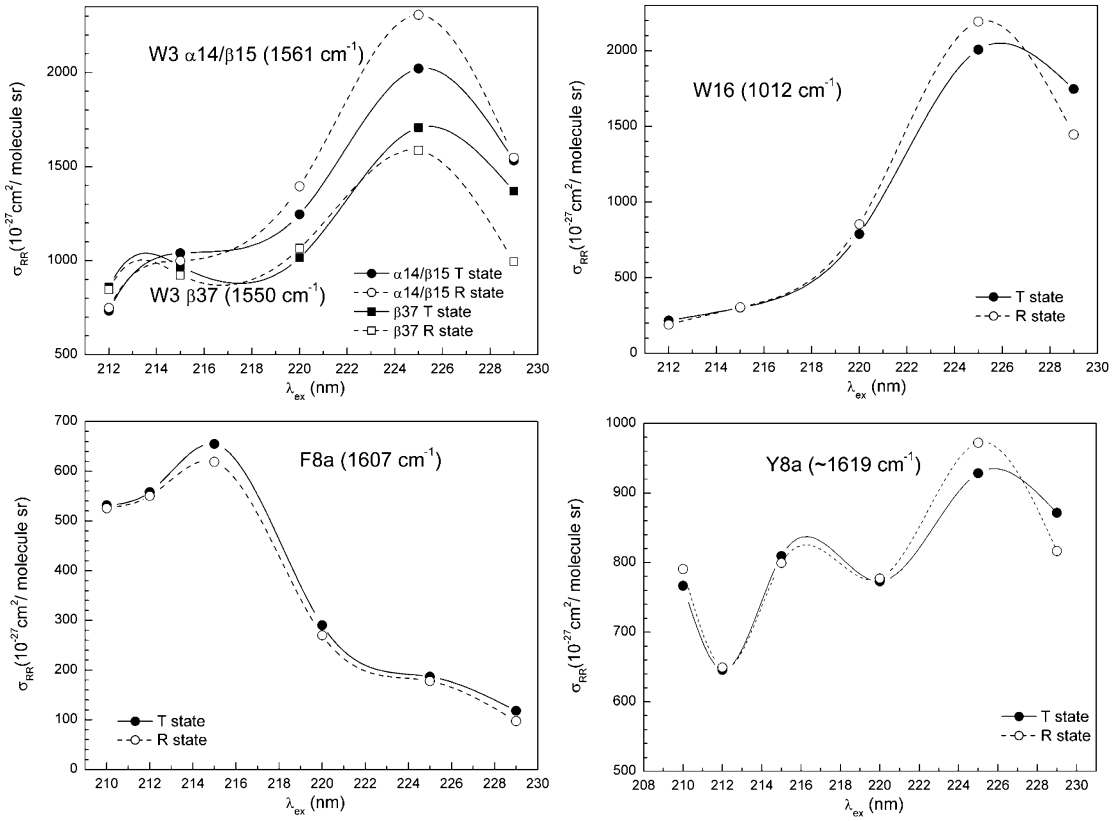


**Figure 2.** Cross-sections of selected aromatic residue bands in hemoglobin spectra as a function of excitation wavelength for CO-bound (R state) and unliganded (T state) HbA.

of the different amino acids (Figure 3). It shows that the largest contribution at 220 nm excitation comes from phenylalanine; the tyrosine bands are weak in comparison (Figure 3). The overlap of Y8a and W1 contributions complicates separation of these bands. However, the width and relative intensity of the deconvoluted W1 component are reasonable compared to other tryptophan bands, and inclusion of the component is crucial to fit the 220 nm Hb spectrum. A significant contribution of W1 to the 220 nm excited spectrum is also reflected by the spectrum of aqueous tryptophan solution (Figure 4).

The T − R difference spectra with 220 nm excitation show positive phenylalanine bands, but also a number of difference bands of tyrosine and tryptophan, especially negative tryptophan bands, such as W16, W7, and the different W3 components (Figure 1).

*Tyrosine.* The frequency upshift of the Y8a mode in the T state, resulting in a characteristic sigmoidal difference feature (maximum at 1622 $cm^{-1}$), is observed with the 220 nm excitation wavelength (Figure 3). It is a probe of H bond formation of tyrosine α42,[1] which accepts a hydrogen bond from Asp$\beta$99, the "switch" contact in the T state, and is also characteristic for the 229 nm excited T − R spectra (Figure 3). A small contribution of the tryptophan W1 mode (1622 $cm^{-1}$) to the positive lobe of the tyrosine feature was shown by isotope studies with excitation at 229 nm.[23] Because of the appreciable enhancement of W1 with 220 nm (Figure 4), it is possible that the positive band at 1622 $cm^{-1}$ results from both a frequency upshift of Y8a and a contribution from W1. The excitation profile of Y8a (Figure 2) does not show a difference in cross-section between the T and R states at 220 nm. This suggests that with 220 nm the observed difference results from a frequency upshift in the T state rather than changes in intensity. At 225 and 229 nm excitation, the Y8a cross-sections between T and R differ in addition to the frequency shift. The effect of the shift is diminished by a negative T − R intensity with 225 nm, and positively enhanced for 229 nm, where the Y8a cross-section in T is higher than that in R (compare Figure 2 and difference spectra in Figure 1). Studies with isotope hybrid rHb containing deuterated tyrosine (Tyr-d4) demonstrated that the frequency upshift in the T state is caused by the α-subunit, while the increase in intensity results from changes in the $\beta$-subunit.[23]

*Phenylalanine.* Prominent features of the T − R difference spectrum with 220 nm excitation are the positive bands for the F8a and F8b phenylalanine modes (1607 and 1587 $cm^{-1}$) (Figure 3). Although the differences in F8a for the T and R states are similar for excitations between 220 and 229 nm, F8a cross-section decreases further in both parent spectra with increasing excitation wavelength (Figure 2). The greater influence of the Y8a component and its difference in cross-section between the T and R states result in a weaker appearance of the positive phenylalanine difference bands for 225 nm compared to the one resulting from 220 nm excitation (Figure 1). The 229 nm T − R spectrum shows no differences for F8a/F8b (Figure 3).

*Histidine*. We find a positive band at 1575 $cm^{-1}$ in the 220 nm difference spectra (Figure 3). In a previous experiment with 212 nm excitation, such a band had been observed in a T − R spectrum where no specific assignment could be made, but the contribution of either the tryptophan W2 mode or histidine was suspected.[22] In the 220 nm spectra of aqueous tryptophan the W2 band appears only very weakly (Figure 4); therefore, histidine is more likely the source of the 1575 $cm^{-1}$ difference band here. Recent crystallographic data suggest a movement and weakening of the $\beta_2$His97-$\alpha_1$Thr38 hydrogen bond for the R state,[25] and the change in environment of this or other histidine residues could lead to an altered histidine band.

*Tryptophan.* The UVRR spectra excited between 220 and 229 nm display a strong W3 tryptophan band (Figure 1), which has

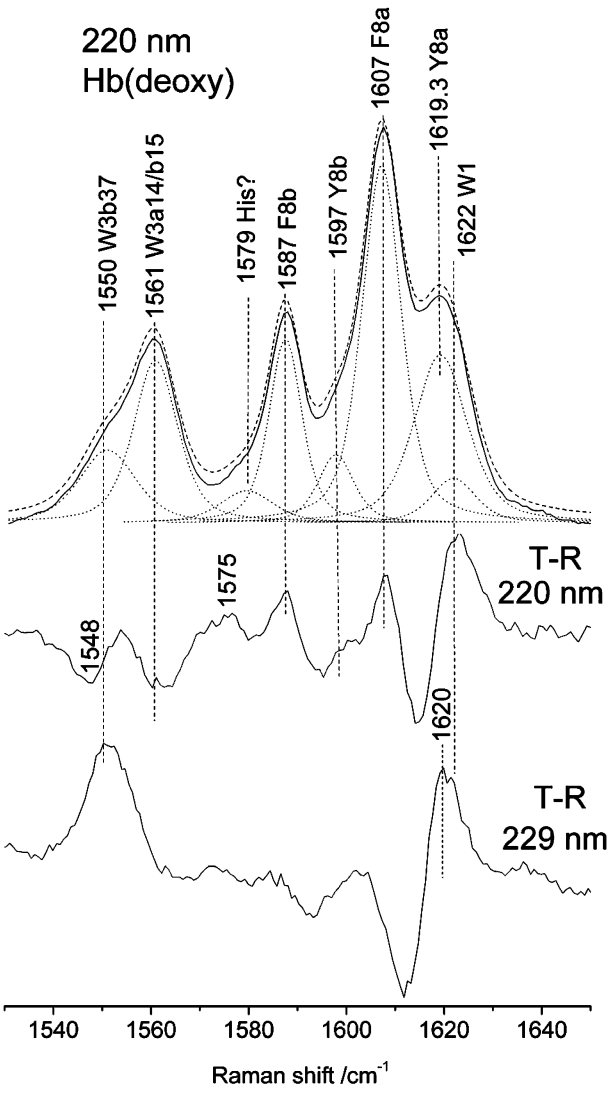


**Figure 3.** RR spectral deconvolution between 1530 and 1650 $cm^{-1}$ for Hb(deoxy) with 220 nm excitation. The reconstructed spectrum trace (dashed line) is slightly displaced from the original spectrum for display purposes. The number of bands and bandwidths were determined from those in 220 nm excited RR spectra of aromatic acids in aqueous solution (compare Figure 4) and found to agree well with the widths in HbA. The bandwidths were kept fixed. Shown below are the T − R difference spectra in the same spectral region with 220 and 229 nm excitation.

two components in Hb, resulting from different tryptophan residues a low-frequency component (1550 $cm^{-1}$) due to W$\beta$37, visible as a shoulder on a high-frequency (1561 $cm^{-1}$) band due to W$\alpha$14 and W$\beta$15 (Figure 3). Assignment of these components was established by isotopic labeling of the residues.[23] The W3 frequency was found to depend on the dihedral angle about the indole-$C_\beta$ bond, which is smaller for W$\beta$37.[26] The excitation profiles of the different W3 components in the deoxy and the CO-liganded state of Hb elucidate major differences in the T − R spectra with 229 and 220 nm excitation (Figure 2). The excitation profiles of both components are slightly red shifted compared to those reported for tryptophan in solution.[12,14]

The cross-sections of W3 of $\alpha$14/$\beta$15, which act as H bond donors to the intrasubunit residues Thr$\alpha$67 and Ser$\beta$72, respectively, are equal for both the high and low affinity states with 229 nm excitation (Figure 2), so that no T − R difference band is observed at this position (Figure 3). This was also found in previous studies of Hb at 229 nm and led to the assumption

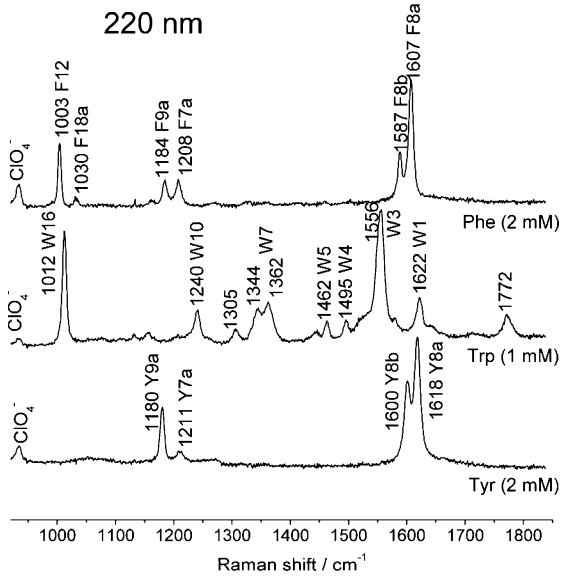


**Figure 4.** Resonance Raman spectra of aqueous tyrosine, tryptophan, and phenylalanine excited with 220 nm.

that there is no significant change in the H bond strength between the T and R states. The H bond acceptors of Trp$\alpha$14/$\beta$15 are the same for the low and the high affinity states.[5,23] Unlike with 229 nm excitation, however, the cross-section of their W3 (1561 $cm^{-1}$) component is higher for the R state than for the T state when excited with 225 and 220 nm (Figure 2). The R state excitation profile is also slightly blue shifted. Both cause a negative difference band at 1561 $cm^{-1}$ (Figure 3). The difference signal of Trp$\alpha$14/Trp$\beta$15 suggests different strengths of the H bonds of one or both of these residues, with weaker H bond interaction in the R state. Thus, due to the now known excitation profiles of both states, the interpretation drawn from the 229 nm spectra needs modification.

The cross-section of W3$\alpha$14/$\beta$15 in the T state is generally lower than in R throughout the excitation profile (Figure 2). For some model compounds, it could be shown that the interaction of cations with the $\pi$-conjugated indol ring of tryptophan can reduce the cross-section in Raman bands that are in resonance with the 220 nm Trp absorption band.[27] In a complex system such as a protein, cationic amino acid residues could induce such an effect. However, the crystal structures of hemoglobin in the two affinity states show no evidence of cationic amino acid side chains (lysine, arginine, or histidine) in the proximity of the $\alpha$14/$\beta$15 indole rings. Therefore, it seems more likely indeed that altered H bond interactions lead to the observed changes in the T state excitation profile.

The distances of W$\alpha$14/$\beta$15 to their H bond acceptors were found to vary between crystal structures of the ligand-bound state obtained under crystallization in high[25,28] and low[29] salt concentration (referred to as R and R2, respectively), also summarized by Balakrishnan et al.[8] recently. While the crystallographic data of R2 (1.70 Å resolution,[29]) give (Trp)N···O(Thr/Ser) distances for $\alpha$ and $\beta$ chains similar to those of the T state (1.74 Å resolution,[30]), recent data obtained on R (1.25 Å[28] and 2.16 Å resolution[25]) suggest much longer distances (5.33 and 4.10 Å, respectively) in the $\alpha$-subunit. These long distances in the $\alpha$-chains do not allow H bond interactions for Trp$\alpha$14, leaving only the Trp$\beta$15 residues H bonded in the R state. The distances in the $\beta$-chain are similar for the R and R2 structures. A recent study on Thr$\alpha$67 mutants, which are unable to form the Trp$\alpha$14···Thr$\alpha$67 H bond, yielded the same intensity loss for the T and R states, indicating equivalent bonds for both

forms. This, therefore, suggested that the solution structure of HbCO resembled the R2 crystal structure.[8] However, the data presented here imply a change in H bond strength between T and R with a decrease for R, which suggests similarity of HbCO in solution with the R crystal structures.[25,28]

Trp$\beta$37 is known to interact with Asp$\alpha$94 on the $\alpha_1\beta_2$ and $\alpha_2\beta_1$ subunit interfaces through a stronger H bond in the T state than it does with Asp$\beta$102 in the R state. This causes a red shift of its excitation profile for the T state (Figure 2) and hence the strong positive difference band with 229 nm excitation, as well as a negative difference found for 220 nm spectra (Figure 3).

The excitation profile of W16 parallels that of W3$\beta$37 with a slight red shift for the T state; the W16 difference is positive for 229 nm excitation and negative for 220 nm (Figure 2). Crossing of the profiles occurs between 229 and 225 nm, yielding a negative difference for W16 with 225 nm excitation (Figure 1). A comparison of the W16 cross-sections in Hb with those in tryptophan solution reveals that the cross-section is decreased in Hb, along with a red shift of the excitation profile.[12]

**3.2. Monitoring the HbCO Photocycle with 220 nm.** Since the phenylalanine residues in Hb can be probed very well by means of the positive T − R signal from F8a and F8b with 220 nm excitation, along with tyrosine and tryptophan, we explored their evolution in time-resolved (photodeligation) experiments with 220 nm excitation. RR spectra with 220 nm excitation were acquired at different time points after photodeligation of CO from HbCO by a 419 nm pump pulse from a second laser (see the Methods section for details).

Figure 5 displays the difference spectra between the spectra taken after the pump pulse and the HbCO spectrum for different time delays. The phenylalanine bands F8a and F8b (1607 $cm^{-1}$ and 1587 $cm^{-1}$) are visible from 40 ns on. They become slightly more intense for longer delay times, increasing from approximately 2% at 40 ns until they reach around 4% of their intensity in HbCO at 50 $\mu$s. Around 2.5 $\mu$s, the difference spectra start to contain a sigmoidal band due to the shift of the Y8a tyrosine mode to higher frequency and the positive lobe at 1622 $cm^{-1}$ associated with this shift. Throughout the photocycle the difference spectra reveal mainly negative tryptophan features: Aside from W3($\alpha$14/$\beta$15) and W16, the W7 Fermi doublet bands (1343 and 1367 $cm^{-1}$) are also negative and become more pronounced with increasing delay time. A very interesting feature probably characteristic for the T state, since it starts to appear in the 20 $\mu$s spectra, is the negative difference for the W3 $\beta$37 component, as discussed above in context with its excitation profiles and the static spectra.

As found in other time-resolved studies,[9] around 21 $\mu$s after deligation the molecules have reached the T structure, so the difference between the intermediate and the HbCO spectrum resembles the "static" T − R difference spectrum (also shown in Figure 5 for comparison). The intensity difference between the static T − R and the 50 $\mu$s difference spectrum, due to the fact that the signal arises from a smaller population of molecules in the time-resolved experiments than in the static experiments (approximately 50%) as a result of geminate recombination and ligand distribution among Hb molecules, was discussed previously.[9]

**3.3. Spectra of the HbCO Photocycle Intermediates.** Time-resolved studies with 229 nm excitation monitor the breaking and formation of H bonds during the HbCO photocycle by probing the tyrosine and tryptophan residues involved in H bond quaternary contacts. Fitting of the deconvoluted difference bands to a series of exponentials revealed five time constants, which were assigned to different intermediates in the photocycle (Figure 6A).[9]

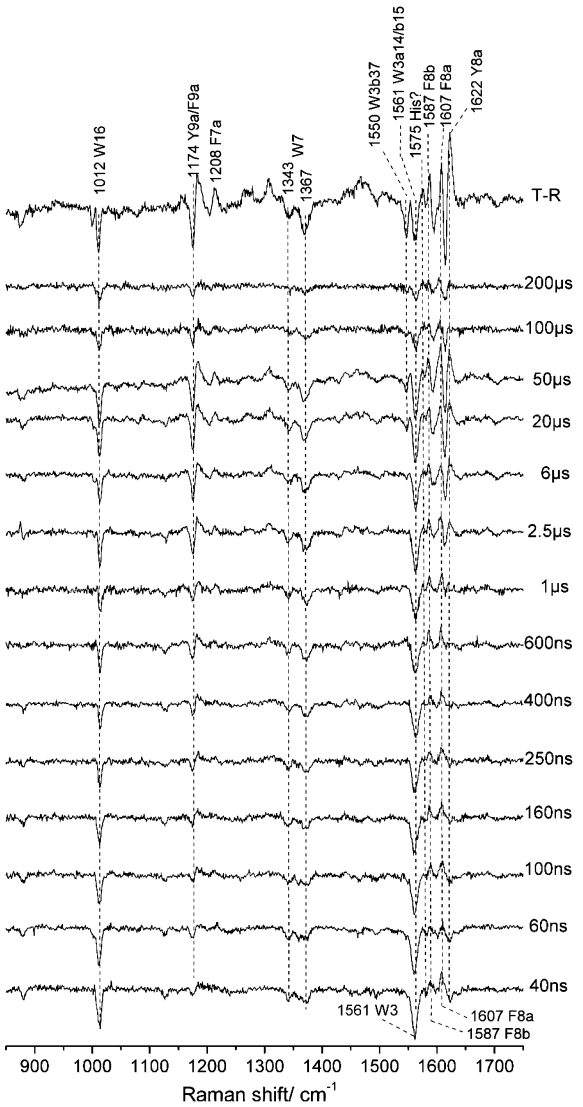


**Figure 5.** Difference RR spectra (probe only minus pump−probe) at 220 nm excitation for different delay times after photodeligation; the T − R static spectrum is shown at the top for comparison.

We found that the same UVRR bands that made identification of the photocycle intermediates and extraction of the time constants possible, and exhibited identical consistent kinetics, show a different evolution in 220 nm experiments. Since the data per se are not very informative, we display only a few examples in Figure 6B to illustrate that reproduction of the actual HbCO kinetics and observation of dynamics is more complicated with 220 nm excitation. The dashed lines in Figure 6B show the best fit that can be achieved with the rate constants extracted for the respective bands in 229 nm experiments (table in Balakrishnan et al.[9]). We find that the overall time courses can be matched, although the amplitudes of the individual terms differ greatly from those in 229 nm experiments.

To learn more about the difference signature of the 220 nm excited photocycle intermediates, we calculated individual spectra of the intermediates using the known rate constants (Figure 6A). Figure 7 compares these spectra (Figure 7A) with those obtained from the experiment with 229 nm excitation, where the spectral characteristics of the intermediates could be interpreted in terms of contact formation during the R−T transition[9] (Figure 7B).

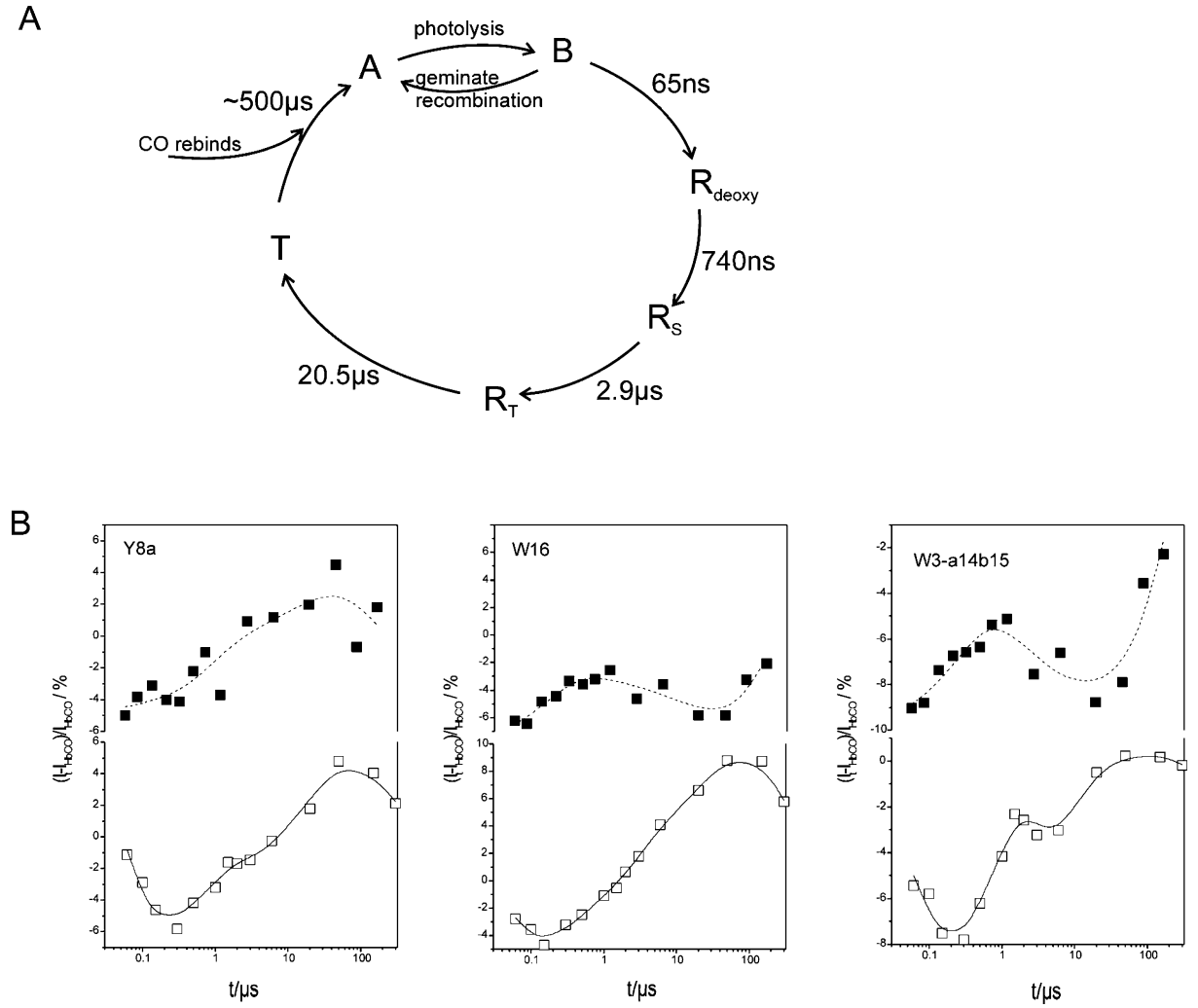


**Figure 6.** (A) Scheme for the successive intermediates in the HbCO photocycle as determined from UVRR experiments at 229 nm.[9] (B) Logarithmic time plots of the relative difference intensities for selected bands Y8a, W16, and W3(α14/$\beta$15) extracted from the time-resolved data (filled squares). The dashed lines indicate the best fit obtained with the time constants that resulted from experiments with 229 nm excitation, reproduced below (open squares and solid lines, from ref 9).

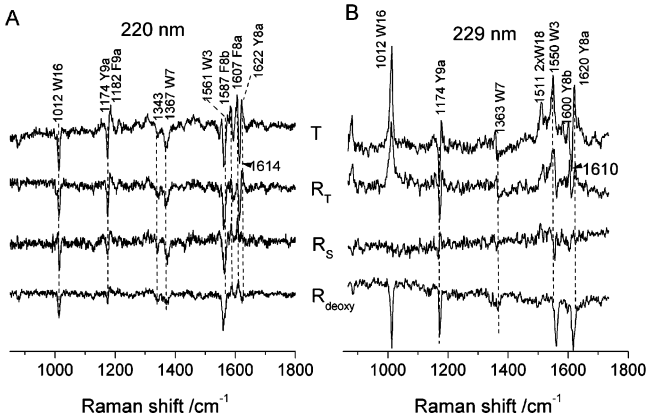


**Figure 7.** (A) Computed difference spectra obtained with 220 nm excitation wavelength for the successive intermediates in the HbCO photocycle. (B) Difference spectra obtained with 229 nm excitation (adapted from Balakrishnan et al.[9]).

The 229 nm excited spectrum of the earliest intermediate, $R_{deoxy}$, shows negative bands for the Y8a tyrosine and the W3 α14/$\beta$15 and W16 tryptophan modes. They were proposed to result from the breaking of the interhelical H bonds between the A−E (Trpα14/$\beta$15) and H−F (Tyrα140/$\beta$145) helices due to rotation of the E and F helices upon deligation of CO. These bonds are restored in the second intermediate $R_S$, which therefore shows no difference features. In the $R_T$ intermediate, the "hinge" contact, namely the H bond of Trp$\beta$37 with Aspα94, is formed at the $\alpha_1\beta_2$ and $\alpha_2\beta_1$ interfaces, which is indicated by a positive difference signal for the $\beta$37 component of W3. Finally, the T state is reached by formation of the "switch" contact between Tyrα42 and Asp$\beta$99, leading to the clear frequency upshift of Y8a.[9]

The intermediate spectra obtained in our 220 nm experiment are different from the 229 nm spectra. The negative tyrosine features at the Y8a position and also for Y9a, both indicative of the H bond breakage between the H and F helices, are very weak in the $R_{deoxy}$ spectrum. Although an explanation of this effect has to remain speculative, we assume crossing of the Y8a excitation profiles of R and $R_{deoxy}$ species around this wavelength, resulting in a very small or no difference. In addition, the positive difference bands for phenylalanine (F8a/F8b) appearing in this early intermediate probably overlap with a negative tyrosine signal. Nevertheless, the Y8a shift characteristic of tyrosine α42 hydrogen bond formation when the molecule moves toward the T state is clearly seen at 220 nm, as well as for the 229 nm excitation in the $R_T$ and T spectra.

The strong negative W3 and W16 signals of Wα14/$\beta$15 in $R_{deoxy}$ are similar to the differences seen with 229 nm, indicating that the intensity loss upon breaking of the interhelical H bonds

**TABLE 1: Intensity Difference of the F8a and F8b Bands for Different Photocycle Intermediates as Percent of Its Intensity in HbCO**

| photocycle intermediate | $I_t - I_{HbCO}/I_{HbCO}$ in % | |
|---|---|---|
| | F8a (1607 $cm^{-1}$) | F8b (1587 $cm^{-1}$) |
| $R_{deoxy}$ | 1.4 | 1.9 |
| $R_S$ | 1.7 | 3.0 |
| $R_T$ | 1.8 | 3.3 |
| T | 2.3 | 3.7 |

of Trpα14 with Thrα67 and Trp$\beta$15 with Ser$\beta$72 is observed at both wavelengths. However, unlike the absence of difference signals observed for $R_S$ with 229 nm excitation, which has been interpreted as being indicative of H bond restoration at this stage, the negative bands are still present in the spectra of the $R_S$ intermediate when excited with 220 nm. This suggests that the Trp H bonds may have reformed, but that the extent to which this process has taken place and/or the strength of the reformed bonds are different compared to the R state. The W3α14/$\beta$15 band remains negative throughout the photocycle. We ascribe this effect to two different causes: First, breaking of the internal H bonds causes a negative signal for the $R_{deoxy}$ intermediate, and bond reforming, although possibly to a different extent, occurs in the $R_S$ intermediate. Second, for the later intermediates $R_T$ and T, an additional process, which leads to the smaller cross-section in the T state (compare the excitation profile in Figure 2), possibly due to weaker H bonding in the R state as discussed above, replaces the initial observation of H bond breaking and reforming. Unlike with 229 nm excitation, where $R_T$ and T are dominated by the positive W3$\beta$37 difference band, only the internal tryptophan residues α14/$\beta$15 produce significant signal throughout the whole R to T transition. In accordance with the excitation profile (Figure 2), a slightly negative difference for W3$\beta$37 appears in the $R_T$ and T intermediates. The kinetic behavior of W16 parallels that of the α14/$\beta$15 W3 component (compare middle and right plot in Figure 6B), while in the 229 nm study the evolution showed more similarities with that of W3 $\beta$37 (Figure 8 of Balakrishnan et al.[9]), suggesting that, for W16 as well as for W3, the T and R excitation profiles cross around 220 nm for Trp$\beta$37.

**3.4. Probing Phenylalanine.** The time-resolved RR spectra discussed so far made clear that the strong positive phenylalanine bands found in static Hb(deoxy)−Hb(CO) experiments with 220 nm are not only characteristic of the T state, but that they are seen from the early intermediates on (40 ns) (Figure 7A). The immediate intensity change is followed by a slow evolution and shows a clear increase with longer delay time (Table 1). The relative changes compared to the intensity of the bands in the HbCO spectrum appear higher in F8b than those for F8a, although the cross-section of F8b is weaker (e.g., Figure 3). This can be attributed to the overlap of a positive difference signal for F8a with the negative lobe caused by the frequency upshift of Y8a. Compared with the changes other difference bands undergo during the photocycle, such as the tyrosine or the tryptophan modes (Figure 6B), the changes seen in the phenylalanine difference are relatively small.

Both the early appearance of the phenylalanine signals after photodeligation and the persistence of more or less the same positive difference feature suggest that they have to do directly with the removal of the CO ligand from the Hb molecule and changes occurring at the heme. Each α$\beta$ dimer of HbA contains 15 phenylalanine residues, some of which are highly conserved and known to be in proximity to the heme. These are Pheα43/$\beta$42 (position CD1) and Pheα98/$\beta$103 (position G5), located on opposite sides of the heme plane, respectively. Most of the known Phe$\beta$42 mutants exhibit lowered $O_2$ affinity, lower cooperativity, and/or are less stable than the wild type.[31−33] Residue $\beta$42/α43 (position CD1) is directly packed against the heme (Figure 8), and has contact with the ligand. Removal of the ligand (breaking of the Fe−CO bond) leads to electronic reorganization of the porphyrin ring as the $Fe^{2+}$ converts from a low to a high spin state. This process takes place within femtoseconds to picoseconds.[34,35] It is reasonable that a change in environment of the CD1 phenylalanine residues induced by these processes could lead to the observed increase in Raman signal. The modest additional intensification for the later intermediates (Table 1) may reflect rearrangements in the vicinity of the heme. For example, the closest distance from Phe$\beta$42 to one of the heme propionate oxygen atoms diminishes from 7 to 8 Å in the R and $R_2$ crystal structures to 5.9 Å in the

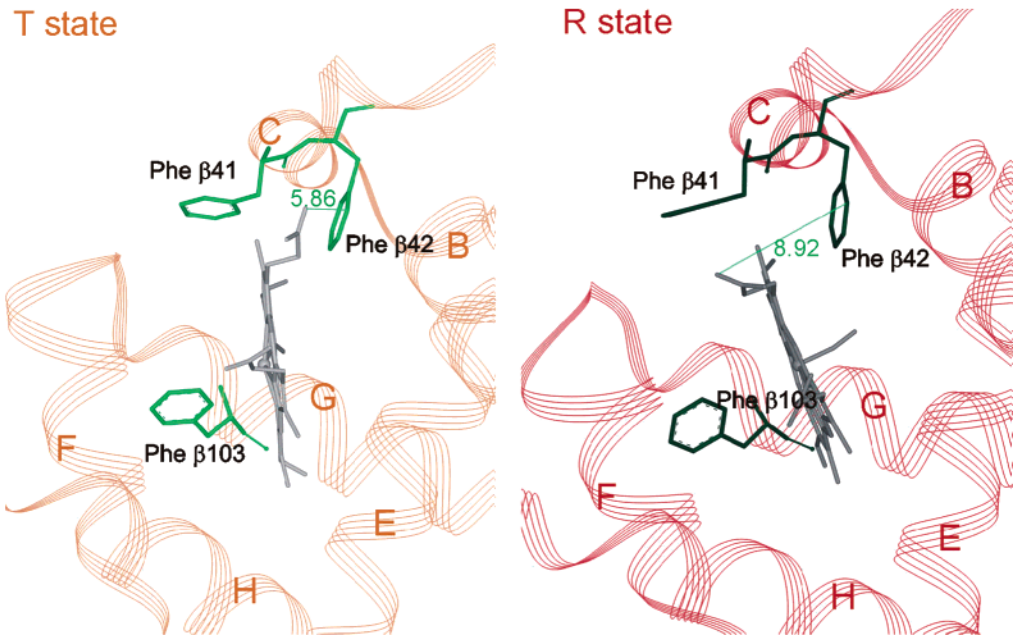


**Figure 8.** Phenylalanine residues CD1 ($\beta$42) and G5 ($\beta$103) in the T and R structures (coordinates obtained from the crystal structures 2HHB[30] and 1IRD[28] from the Brookhaven Protein Data Base).

T state (crystallographic coordinates from Park and Tame[28] and Fermi et al.[30]); the resulting electrostatic effect could contribute to the F8a/F8b intensification.

## Conclusions

The UVRR spectra of Hb change markedly with changing excitation wavelengths, due to differential enhancement of amide and aromatic residue vibrational modes. However, the Hb(deoxy)/HbCO difference spectra reveal only weak features for wavelengths below 220 nm, indicating few useful markers of structure change in this region. With 220 nm excitation, large difference signals are observed, comparable to those seen with 229 nm excitation but different in character. Time-resolved UVRR spectra at 220 nm reveal prompt changes in phenylalanine signals, suggesting that the Phe residues in the heme pocket sense the electronic effects of ligand dissociation. Continuing evolution of the Phe difference signals may reflect structural rearrangement in the heme pocket along the allosteric coordinate.

The tryptophan and tyrosine difference signals evolve differently at 220 than at 229 nm, reflecting altered excitation profiles of Trp and Tyr residues in the T and R states. A major new finding is that the Trp$\alpha$14···Ser$\alpha$67 and Trp$\beta$15···Thr$\beta$72 H bonds have different strengths in the T and R states, despite the absence of a T − R difference signal for these interior Trp residues at 229 nm, where the excitation profiles happen to coincide. It remains the case that these H bonds are broken in the earliest photocycle intermediate, $R_{deoxy}$, but subsequent protein motions reestablish H bonds that are weaker than the initial R state H bonds.

**Acknowledgment.** We thank Radhika Rajendran for providing software to facilitate calculation of the Raman cross-sections. This work was supported by the National Institute of Health (Grant No. GM 25158).

## References and Notes

(1) Rodgers, K. J.; Su, C.; Subramaniam, S.; Spiro, T. G. *J. Am. Chem. Soc.* **1992**, *114*, 3697.
(2) Jayaraman, V.; Rodgers, K. R.; Mukerji, I.; Spiro, T. G. *Science* **1995**, *269*, 1843.
(3) Peterson, E. S.; Friedman, J. M. *Biochemistry* **1998**, *37*, 4346.
(4) Hu, X. H.; Rodgers, K. R.; Mukerji, I.; Spiro, T. G. *Biochemistry* **1999**, *38*, 3462.
(5) Wang, D. J.; Zhao, X. J.; Shen, T. J.; Ho, C.; Spiro, T. G. *J. Am. Chem. Soc.* **1999**, *121*, 11197.
(6) Nagai, M.; Wajcman, H.; Lahary, A.; Nakatsukasa, T.; Nagatomo, S.; Kitagawa, T. *Biochemistry* **1999**, *38*, 1243.
(7) Juszczak, L.; Fablet, C.; Baudin-Creuza, V.; Lesecq-Le Gall, S.; Hirsch, R.; Nagel, R.; Friedman, J. M.; Pagnier, J. *J. Biol. Chem.* **2003**, *278*, 7257.
(8) Balakrishnan, G.; Tsai, C. H.; Wu, Q.; Case, M. A.; Pevsner, A.; McLendon, G. L.; Ho, C.; Spiro, T. G. *J. Mol. Biol.* **2004**, *340*, 857.
(9) Balakrishnan, G.; Case, M. A.; Pevsner, A.; Zhao, X. J.; Tengroth, C.; McLendon, G. L.; Spiro, T. G. *J. Mol. Biol.* **2004**, *340*, 843.
(10) Kaminaka, S.; Ogura, T.; Kitagawa, T. *J. Am. Chem. Soc.* **1990**, *112*, 23.
(11) Antonini, E.; Brunori, M. *Hemoglobin and Myoglobin in their Reactions with Ligands*; North-Holland Publishing Company: Amsterdam, 1971.
(12) Zhao, X.; CHen, R.; Tengroth, C.; Spiro, T. G. *Appl. Spectrosc.* **1999**, *53*, 1200.
(13) Asher, S. A.; Ludwig, M.; Johnson, C. R. *J. Am. Chem. Soc.* **1986**, *108*, 3186.
(14) Fodor, S.; Copeland, R.; Grygon, C.; Spiro, T. G. *J. Am. Chem. Soc.* **1989**, *111*, 5509.
(15) Chang, S.; Yang, W.; Spiro, T. G. *J. Raman Spectrosc.* **1990**, *21*, 435.
(16) Rava, R. P.; Spiro, T. G. *J. Phys. Chem.* **1985**, *89*, 1856.
(17) Siamwiza, M. N.; Lord, R. C.; Chen, M. C.; Takamatsu, T.; Harada, I.; Matsuura, H.; Shimanouchi, T. *Biochemistry* **1975**, *14*, 4870.
(18) Hildebrandt, P. G.; Copeland, R. A.; Spiro, T. G.; Otlewski, J.; Laskowski, M.; Prendergast, F. G. *Biochemistry* **1988**, *27*, 5426.
(19) Thomas, G. J., Jr. *Biopolymers* **2002**, *67*, 214.
(20) Chen, R. P.; Spiro, T. G. *J. Phys. Chem. A* **2002**, *106*, 3413.
(21) Jordan, T.; Mukerji, I.; Wang, Y.; Spiro, T. G. *J. Mol. Struct.* **1996**, *379*, 51.
(22) Zhao, X. J.; Spiro, T. G. *J. Raman Spectrosc.* **1998**, *29*, 49.
(23) Hu, X.; Spiro, T. G. *Biochemistry* **1997**, *36*, 15701.
(24) Zhao, X. J.; Chen, R. P.; Raj, V.; Spiro, T. G. *Biopolymers* **2001**, *62*, 158.
(25) Safo, M. K.; Burnett, J. C.; Musayev, F. N.; Nokuri, S.; Abraham, D. J. *Acta Crystallogr., Sect. D* **2002**, *58*, 2031.
(26) Miura, T.; Takeuchi, H.; Harada, I. *J. Raman Spectrosc.* **1989**, *20*, 667.
(27) Takeuchi, H. *Biopolymers* **2003**, *72*, 305.
(28) Park, S.; Tame, J. R. H. *RCSB Protein Data Bank*; 2001, PDB ID 1IRD.
(29) Silva, M. M.; Rogers, P. H.; Arnone, A. *J. Biol. Chem.* **1992**, *267*, 17248.
(30) Fermi, G.; Perutz, M. F.; Shaanan, B.; Fourme, R. *J. Mol. Biol.* **1984**, *175*, 159.
(31) Honig, G. R.; Vida, L. N.; Rosenblum, B. B.; Perutz, M. F.; Fermi, G. *J. Biol. Chem.* **1990**, *265*, 126.
(32) Griffon, N.; Badens, C.; Lena-Russo, D.; Kister, J.; Bardakdjian, J.; Wajcman, H.; Marden, M. C.; Poyart, C. *J. Biol. Chem.* **1996**, *271*, 25916.
(33) Ogata, K.; Ito, T.; Okazaki, T.; Dan, K.; Nomura, T.; Nozawa, Y.; Kajita, A. *Hemoglobin* **1986**, *10*, 469.
(34) Findsen, E. W.; Friedman, J. M.; Ondrias, M. R.; Simon, S. R. *Science* **1985**, *229*, 661.
(35) Franzen, S.; Kiger, L.; Poyart, C.; Martin, J. L. *Biophys J.* **2001**, *80*, 2372.